

Redox Potential Inversion by Ionic Hydrogen Bonding between Phenylenediamines and Pyridines

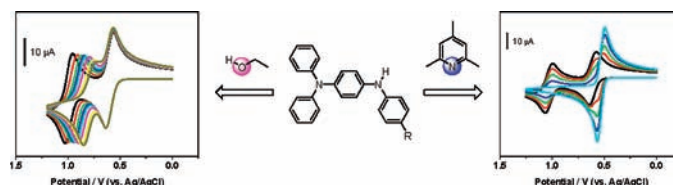
Yi-Chun Chung,[†] Yi-Jung Tu,[†] Shih-Hua Lu,[†] Wan-Chi Hsu,[†] Kuo Yuan Chiu,[†] and Yuhlong Oliver Su^{*,†,‡}

Department of Applied Chemistry, National Chi Nan University, 1 University Road, Puli, Nantou, Taiwan 545, and Department of Materials Science and Engineering, National Chung Hsing University, 250, Kuo Kuang Road, Taichung, Taiwan 402

ysu@nchu.edu.tw

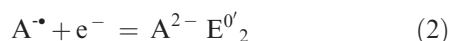
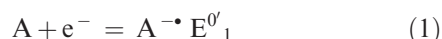
Received March 24, 2011

ABSTRACT



In electrochemical oxidations, the second oxidation potential of phenylenediamines (PD) varies because of hydrogen-bonding formation for PD⁺ with pyridines. A linear relationship was obtained for the potential shift as a function of pK_a of the protonated pyridines and potential inversion could be observed. The oxidized PD⁺ could also form hydrogen bonding with alcohols and the shift of potential exhibits a different pattern.

Many organic compounds may undergo reduction reactions in two steps to form the anion radical first and then the dianion.



Usually the second reduction occurs at a potential more negative than the first one due to electrostatic repulsion. The situation where $E_1^{0'} > E_2^{0'}$ is called “normal ordering of reduction potential”. On the other hand, a process when the second reduction takes place easier than the first one (i.e., $E_1^{0'} < E_2^{0'}$) is referred to as “potential inversion”^{1–3} and characterized as a single two-electron wave. Generally, such an “inverted” order is very rare and occurs mostly

when there is a significant structural change¹ or large solvation² or ion-pairing³ that is coupled with one or two electron-transfer steps.

Electrochemically induced hydrogen bonding had been mainly on the reductive aspect of carbonyl⁴ and nitro^{5–9} compounds. Research groups of Linschitz⁴ and Smith^{5–9} made important contributions in this area. Their work elucidates the interaction between the reduced form of electron-affinitive compounds with hydrogen donors such as alcohol, amides, ureas, etc. The interaction could be monitored by cyclic voltammetry (CV), and digital simulation was used to estimate the formation constants. In the oxidative aspect, metallocenes had been used to form a complex with anions.¹⁰ The hydrogen-bond strength was predicted

[†] National Chi Nan University.

[‡] National Chung Hsing University.

(1) (a) Evans, D. H.; Hu, K. *J. Chem. Soc., Faraday Trans.* **1996**, *92*, 3983–3990. (b) Macias-Ruvalcaba, N. A.; Evans, D. H. *J. Phys. Chem. B* **2006**, *110*, 5155–5160. (c) Lord, R. L.; Schultz, F. A.; Baik, M.-H. *Inorg. Chem.* **2010**, *49*, 4611–4619.

(2) Hapiot, P.; Kispert, L. D.; Konovalov, V. V.; Savéant, J.-M. *J. Am. Chem. Soc.* **2001**, *123*, 6669–6677.

(3) (a) Nafady, A.; Chin, T. T.; Geiger, W. E. *Organometallics* **2006**, *25*, 1654–1663. (b) Macias-Ruvalcaba, N. A.; Evans, D. H. *J. Phys. Chem. B* **2005**, *109*, 14642–14647.

(4) Gupta, N.; Linschitz, H. *J. Am. Chem. Soc.* **1997**, *119*, 6384–6391.

(5) Ge, Y.; Lilienthal, R. R.; Smith, D. K. *J. Am. Chem. Soc.* **1996**, *118*, 3976–3977.

(6) Ge, Y.; Smith, D. K. *Anal. Chem.* **2000**, *72*, 1860–1865.

(7) Ge, Y.; Miller, L.; Ouimet, T.; Smith, D. K. *J. Org. Chem.* **2000**, *65*, 8831–8838.

(8) Bu, J.; Lilienthal, N. D.; Woods, J. E.; Nohrden, C. E.; Hoang, K. T.; Truong, D.; Smith, D. K. *J. Am. Chem. Soc.* **2005**, *127*, 6423–6429.

(9) Chan-Leonor, C.; Martin, S. L.; Smith, D. K. *J. Org. Chem.* **2005**, *70*, 10817–10822.

from acid–base molecular properties by using the pK_a slide rule.¹¹

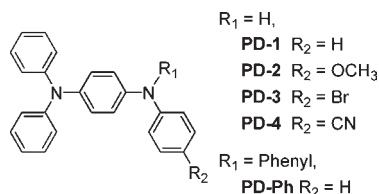


Figure 1. Structure of substituted phenylenediamines.

To our knowledge, however, there is no example found to invert the potential order through changes in H-bonding strength. In this paper, we report the ionic hydrogen bonding^{12,13} formation through electrooxidation of a series of *p*-phenylenediamines (Figure 1) and their interaction with pyridines and alcohols through different patterns. The ionic hydrogen bonding plays a crucial role in stabilizing the oxidation product and hence favors the second oxidation.

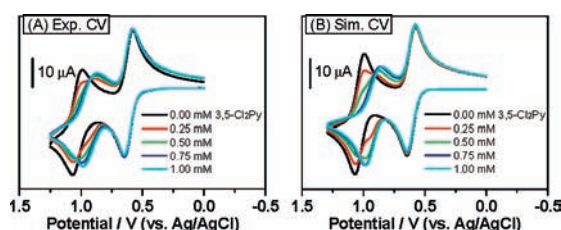


Figure 2. CVs of 1 mM **PD-1** in CH_3CN containing 0.1 M TBAP and various concentration of 3,5- Cl_2Py . Scan rate: 0.1 V/s. Working electrode: glassy carbon disk (area = 0.07 cm^2).

All phenylenediamines (PD) exhibit two reversible oxidation waves in acetonitrile (CH_3CN), corresponding to the formation of radical cation, $\text{PD}^{+\bullet}$, and dication, PD^{2+} . As shown in Figure 2(a), the CV of **PD-1** shows two reversible redox couples at $E_1^{\text{ox}} = +0.61$ V and $E_2^{\text{ox}} = +1.03$ V. As 3,5-dichloropyridine (3,5- Cl_2Py , $pK_a = 0.67$)¹⁴ is added to the solution of **PD-1**, a new oxidation wave (E_2^{ox}) grows between the two original oxidation waves. The first oxidation remains unchanged, and the current of second oxidation at $E_2^{\text{ox}} = +1.03$ V gradually decreases as the 3,5- Cl_2Py concentration increases. When the 3,5- Cl_2Py concentration reaches 1 equiv of **PD-1**, the second oxidation wave completely disappears and the appearance of the new wave on the negative side of the second oxidation wave is thus assigned as the new second oxidation associated with 3,5- Cl_2Py . The new oxidation

wave also exhibits less reversibility than two original waves. Interestingly, when the same experiment is measured with **PD-Ph**, there is no significant difference in wave potential and shape (Figure S1, Supporting Information). This strongly suggests that these differences are caused by a H-bonding interaction between **PD-1**⁺ and 3,5- Cl_2Py . The presence of H-bonding is also supported by UV–vis spectra that exhibit the decrease in the characteristic IVCT band of **PD-1**⁺ after addition of 3,5- Cl_2Py (Figure S9, Supporting Information).

Several pyridines with different substituents, and hence of different pK_a 's, had been investigated for their effect on the electrochemical waves. The new redox potential is closer to the first one as the pyridine derivative has a higher pK_a (Table S1, Supporting Information).

Addition of pyridine produces no potential shift in the first oxidation wave of **PD-1**, indicating no significant interaction between the neutral form and pyridine. The second oxidation in the presence of pyridines, however, results in a significant negative shift in potential and broadening of wave shape. The new redox couple, of which the shift of potential depends on the pK_a of pyridines, gradually moves to a more negative potential and then merges with the first one (Figures S2–S6, Supporting Information)

When 2,4,6-trimethylpyridine (2,4,6- Me_3Py , $pK_a = 7.48$)¹⁴ is added to the solution of **PD-1**, the CV exhibits a different pattern with those for 3,5- Cl_2Py . The new redox couple appears at a potential less positive than that of the first one (Figure 3A). The final CV in the presence of more than 1 equiv of 2,4,6- Me_3Py exhibits only one redox couple at $E_2^{\text{ox}} = +0.53$ V, which is more cathodic than E_1^{ox} . Also, the final peak current is about 1.6 times in magnitude than the first one.

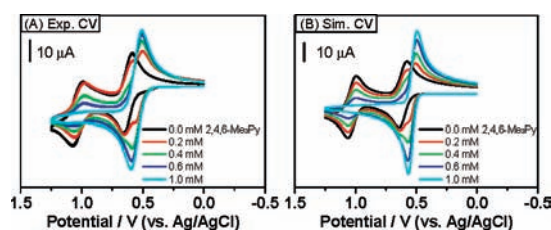


Figure 3. (A) Experimental and (B) simulated CVs of 1 mM **PD-1** in CH_3CN containing 0.1 M TBAP and various concentrations of 2,4,6- Me_3Py . Scan rate: 0.1 V/s. Working electrode: glassy carbon disk (area = 0.07 cm^2).

A plot of ΔE^{ox} as a function of pK_a is thus shown in Figure 4. A linearity with a slope of 57 mV per pK_a indicates the Nernstian relationship^{15a} between the potential shift and the ratio of formation constant for $\text{PD}^{+\bullet}(\text{py})$ and $\text{PD}^{2+}(\text{py})$, i.e., $\log(K_2/K_1)$ and thus significant interaction between the strength of ionic hydrogen bonding can

(11) Gilli, P.; Pretto, L.; Bertolasi, V.; Gilli, G. *Acc. Chem. Res.* **2008**, *42*, 33–44.

(12) Jeffrey, G. A. *An Introduction to Hydrogen Bonding*; Oxford University, 1997.

(13) Mautner, M. *Chem. Rev.* **2005**, *105*, 213–284.

(14) The pK_a of protonated pyridines in water.

(15) See the Supporting Information:(a) pp S9–S10. (b) pp S16–S20. (c) pp S21–S25.

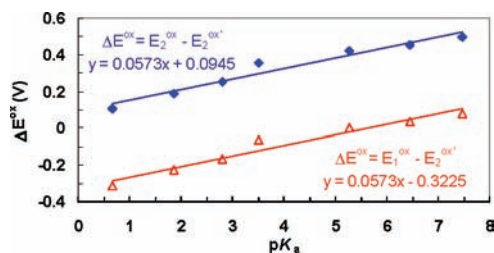
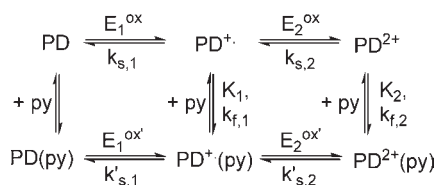


Figure 4. Plots of oxidation potentials difference for PD-1 as a function of pyridines pK_a .

be measured by oxidation potential thermodynamically. As the basicity of the pyridine derivative is higher than 5.62, the E_2^{ox} merged with E_1^{ox} . The new oxidation keeps shifting cathodically in potential as the basicity of pyridine derivatives increases.

We carried out digital simulation of experimental CV using the Digisim 3.03 Program¹⁶ to further understand the redox-dependent H-bonding systems. The reaction mechanism consisting of only electron-transfer and hydrogen bonding equilibria is represented by a six-membered square scheme in Scheme 1.

Scheme 1^a



^a $k_{s,1}$, $k_{s,2}$, $k'_{s,1}$, $k'_{s,2}$: the electron-transfer rate constant (reduction). K_1 , K_2 : formation constants for $\text{PD}^+(\text{py})$ and $\text{PD}^{2+}(\text{py})$ complexes, respectively. $k_{f,1}$, $k_{f,2}$: the forward rate constants for $\text{PD}^+(\text{py})$ and $\text{PD}^{2+}(\text{py})$ complex formation.

The H-bonding equilibrium between neutral PD and pyridines can be eliminated from the scheme due to no significant interaction between them. Two equilibrium constants (K_1 and K_2) and their related kinetic constants ($k_{f,1}$ and $k_{f,2}$) need to be determined. In particular, the determination of the K_1 is quite important because the value of K_1 largely rules the behaviors of the second oxidation which would exhibit two resolved waves or a shifted wave in the presence of pyridines. Thanks to previous models well supported by simulation,¹⁶ some reasonable starting values for different parameters can be used to simulate the reactions suggested in Scheme 1.

It is clear from a qualitative analysis of CV shapes that K_1 cannot be too small, or a shifted wave rather than two separate waves in a second oxidation will be observed.¹⁶ On the other hand, K_2 must be much larger than K_1 in

order to observe negative shift in the second oxidation potential. Because the shift in potential of second oxidation (E_2^{ox} - E_2^{ox}) depends on the ratio of K_2 to K_1 , K_2 is obtained by following eq 3.¹⁶

$$K_2 = K_1 \exp[-nF(E_2^{\text{ox}} - E_2^{\text{ox}})/RT] \quad (3)$$

In the PD/3,5-Cl₂Py system, we set K_1 to be 1000 and then K_2 was calculated to be 1.5×10^5 . Other sets of equilibrium constants in the presence of various pyridines are displayed in Supporting Information. In general, the values of K_1 are in the range of 10^3 – 10^4 M⁻¹.^{15b}

In addition, the forward rates of H-bonding should be very fast so that the shift in potential is effective. In a previous work of Smith, a very rapid value for k_f 's of H-bonding between nitroaniline and 1,3-diphenylurea was in the range of 10^8 – 10^9 M⁻¹ s⁻¹.⁸ In our PD/3,5-Cl₂Py case, the rate constant for $\text{PD}^{+\bullet}$ and pyridine ($k_{f,1}$) is in the range of 10^5 – 10^6 M⁻¹ s⁻¹ and that for PD^{2+} and pyridine ($k_{f,2}$) is approximately the value of 10^8 M⁻¹ s⁻¹ (Figures S11 and S12, Supporting Information). As for the broadening of the new redox waves and decrease in the current magnitude, it is attributed mainly to a rather slow electron-transfer rate ($k'_{s,2}$) for the reduction of $\text{PD}^{2+}(\text{py})$ to $\text{PD}^{+\bullet}(\text{py})$ (Figure S13, Supporting Information), which is hampered by a rapid H-bonding equilibrium between PD^{2+} and pyridine.

With the above consideration, the simulations are able to reproduce the wave shape for most PD/pyridine-binding systems (Figure 2B).^{15b} However, when switching pyridine from 3,5-Cl₂Py to py or 2,4,6-Me₃Py, the second oxidation wave occurs at a more negative potential than the first. Two 1e⁻ oxidation waves of PD coalesce into a single 2e⁻ oxidation wave upon addition of these strongly basic pyridines so that the determination of oxidation potential (E_1^{ox} and E_2^{ox}) and equilibrium constant (K_1 and K_2) becomes quite difficult. Since PD^{2+} is acidic, the proton transfer from PD^{2+} to pyridine or other reactions might happen as the more basic pyridine is present. We tentatively ignore the additional reactions and continue to simulate the CVs of PD in the present of py or 2,4,6-Me₃Py with the same reaction mechanism (i.e., Scheme 1). Satisfactory simulation results are still obtained for potential inversion (Figure 3A,B).

The extremely strong H-bonding between PD^{2+} and 2,4,6-Me₃Py has the effect of *neutralizing* the positive charge on PD^{2+} , which expedites the oxidation of $\text{PD}^{+\bullet}(\text{py})$ to $\text{PD}^{2+}(\text{py})$. Once $\text{PD}^{+\bullet}(\text{py})$ is formed, it is simultaneously oxidized to $\text{PD}^{2+}(\text{py})$. Thus, a 2e⁻ oxidation wave prior to the first original wave grows at the expense of two original waves of unbounded PD.

A different type of behavior in second oxidation is observed upon changing the H-bonding acceptor from pyridine to alcohol (Figure 5A). Stepwise addition of *excess* ethanol (EtOH) can cause the gradual potential shift to the cathodic direction for the second oxidation rather than a new oxidation wave formation while the first oxidation has little change.

To investigate the substituent effect on the H-bonding, the substituted phenylenediamines (Figure 1) are also

(16) Miller, S. R.; Gustowski, D. A.; Chen, Z.-H.; Gokel, G. W.; Echegoyen, L.; Kaifer, A. E. *Anal. Chem.* **1988**, *60*, 2021–2024.

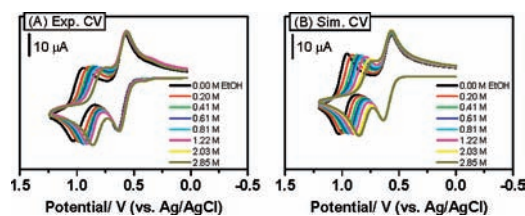


Figure 5. (A) Experimental and (B) simulated CV of 1 mM **PD-1** in CH_3CN containing 0.1 M TBAP and various concentrations of ethanol. $[\text{ethanol}] = 0\text{--}2.85\text{ M}$ overlay. Scan rate: 0.1 V/s. Working electrode: glassy carbon disk (area = 0.07 cm^2).

measured by CV. The CVs appear similar in shape except the difference in redox potential. From these potential shifts for E_2 , we estimate the number (m) of ethanol H-bonded to PD^{2+} and their respective formation constants (K_2) according to eq 4.⁴

$$E_2^{\text{ox}'} = E_2^{\text{ox}} + 0.059 \log(1 + K_2[\text{EtOH}]^m) \quad (4)$$

In this way, it is clear from Figure 6 that estimates of K_2 can reflect the substituent effect on H-bonding of PD^{2+} to

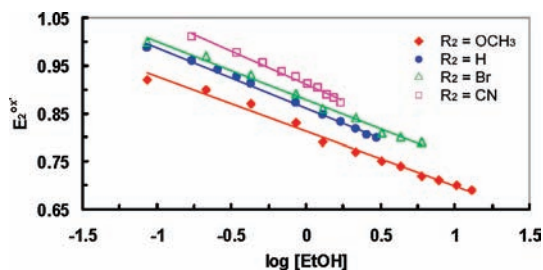


Figure 6. Change of $E_2^{\text{ox}'}$ for **PD-1**, **-2**, **-3**, and **-4** vs $\log [\text{EtOH}]$.

ethanol. The value of K_2 increases as the electron-withdrawing power of the substituent increases. A linearity for $E_2^{\text{ox}'}$ and $\log K_2$ is also observed (Figure S23, Supporting Information). Since ethanol is a very weak base, it takes several ethanol molecules to *neutralize* the positive charge in PD^{2+} . The slopes from Figure 6 give the number (m) of ethanol associated with the dications to be in the range of 1.95–2.58. The values of m , K_2 , and $E_2^{\text{ox}'}$ are listed in Table 1.

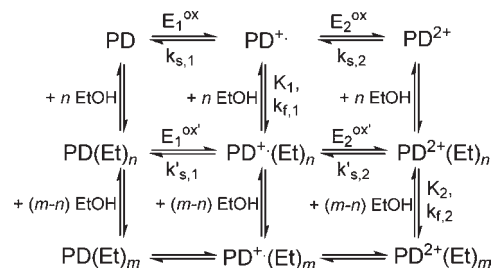
Figure 5B shows the results of simulation for **PD-1** in the presence of ethanol according to the mechanism in Scheme 2 and the parameters in Table 1. We estimate the K_1 to be in

Table 1. Values of the H-Bonded Ethanol Number (m), H-Binding Constant (K_2) to PD^{2+} , and the Redox Potential for Second Oxidation ($E_2^{\text{ox}'}$)

$-\text{R}_2$	m	K_2	$E_2^{\text{ox}'}$	$\log K_2$
$-\text{OCH}_3$	2.13	2.26×10^2	+0.91	1.35
$-\text{H}$	2.58	1.50×10^2	+1.01	2.18
$-\text{Br}$	1.95	2.63×10^2	+1.03	2.42
$-\text{CN}$	2.40	4.21×10^2	+1.06	2.62

the range of $10^{-3}\text{--}10^{-4}\text{ M}^{-1}$ because there is no significant change in the first wave and a single shifted wave in second oxidation is observed.¹⁶ Although K_1 is very small, we expect its corresponding forward rate constant ($k_{f,1}$) to be the large values of $10^8\text{--}10^9\text{ M}^{-1}\text{ s}^{-1}$.^{15c} An excellent agreement between experimental and simulated CV has been obtained (Figure 5).

Scheme 2^a



^a $k_{s,1}$, $k_{s,2}$, $k'_{s,1}$, $k'_{s,2}$: the electron-transfer rate constant (reduction). $k_{f,1}$, $k_{f,2}$: the forward rate constant for H-bonding formation.

In conclusion, we report that the second oxidation wave of PDs varies due to H-bonding interaction with pyridines or alcohol. As 2,4,6- Me_3Py is used as a hydrogen acceptor, the redox potential inversion of **PD-1** occurs. It is possible that the potential inversion by ionic H-bonding would also take place if we change the hydrogen donor and/or acceptor and/or the size of electrolytes.

Acknowledgment. This work was supported by the National Science Council of Republic of China.

Supporting Information Available. Syntheses, experimental and simulated procedures for **PD-1**, **-2**, **-3**, and **-4**, and additional titration data. This material is available free of charge via the Internet at <http://pubs.acs.org>.